SUPPLEMENT MATERIAL

Detailed Methods

Generation of Mice

Sox9$^{flox/flox}$ female mice[1] were bred with *Col2a1-cre* males (Jackson Laboratories)[2] to generate heterozygous offspring (*Sox9*$^{flox/+}$*;Col2a1-cre*) and *Cre* negative Sox9$^{flox/+}$ littermate controls at expected Mendelian ratios. To determine recombination, *Col2a1-cre* mice were crossed with *Rosa26R-lacz* (*Rosa26R*) reporter mice and sacrificed at postnatal day 1. Genotyping was performed by RT-PCR as previously described for adult genomic DNA.[1, 3]

Tissue Preparation

Sox9$^{flox/+}$*;Col2a1-cre* mice and *Sox9*$^{fl/+}$ littermate controls were sacrificed at 3, 6, and 12 months of age. Hearts were removed and fixed in 4% paraformaldehyde overnight at 4°C. Tissue was processed through 10, 20 and 30% sucrose solutions before embedding in OCT freezing compound (Tissue-Tek), and sectioning 10µm-thick. Frozen sections were stored at -20°C and allowed to dry at 42°C for 20 minutes and rinsed in 1XPBS prior to immunohistochemical, in situ hybridization or histological staining.[3] Hearts from E18.5 Col2*a1-cre*;*Rosa26R* mice were fixed in 4% paraformaldehyde overnight at 4°C, embedded in paraffin and sectioned for X-Gal staining as described.[3, 4]

Taqman Low Density Array (TLDA) and Real-Time PCR

RNA was isolated from atrioventricular regions from *Sox9*$^{flox/+}$*;Col2a1-cre* and Sox9$^{fl/+}$ littermate controls at 3, 6, and 12 months of age. 400ng of RNA was subject to cDNA synthesis according to the manufacturer's instructions (Applied Biosystems) and TaqMan Low Density Array (TLDA) or real-time PCR was performed. TLDA cards consist of 384 wells pre-loaded with selected 4 x 96 Taqman oligos including 2 endogenous controls, for high-throughput, low reaction volume, real-time PCR. For each TLDA card, 10µl of each cDNA sample was diluted in 90µl of double distilled water and mixed with 100µl of Taqman master mix (#4304437, Applied Biosystems). Standard recommended PCR protocols were performed (50°C for 2 minutes, 94.5°C for 10 minutes, 97°C for 30 seconds, 59.7°C for 1 minute, with steps 3 and 4 repeated for 40 cycles) using the Applied Biosystems 7900 HT Fast Real-Time PCR System. ΔCT (cycle count to threshold) values were determined by normalization to *18s* using the RQ SDS manager software (Applied Biosystems). For real-time PCR, individual TaqMan inventoried detection assays (Applied Biosystems) were used against chicken *Sox9*, mouse *Sox9*, mouse *Runx2* and mouse *Osteopontin* according to manufacturer's instructions and normalized to*18s* expression levels. Sample wells with a CT of 40 were excluded from analysis as outliers when more than two standard deviations above the mean of replicates. Statistically significant differences in transcript level were determined using Student's t-test or one-way ANOVA with $p<0.05$ considered significant.

Histology and Immunostaining

Tissue sections were prepared as described above and blocked in 10% heat inactivated goat serum, 0.1% Tween-20 in 1xPBS for 1 hour at room temperature. For elastin staining, tissue sections were subject to antigen retrieval by boiling in unmasking solution (Vector Labs) for 10 minutes. Primary antibody incubations (in 1:1 block solution:PBS) were carried out overnight at 4°C at the following dilutions: PECAM (sc1505, Santa Cruz) (1:50), Sox9[5] (1:1000) and Elastin (sc-17581, Santa Cruz) (1:100). Following primary antibody incubation, sections were washed in 1x PBS and incubated with respective anti-rabbit, anti-goat or anti-mouse Alexa 488 or 568 secondary antibodies at 1:400 dilution for 1 hour at room temperature, washed, and incubated with DAPI (blue) for identification of nuclei before mounting in Vectashield (Vector Laboratories). Alternatively for Vcam-1 detection, colorimetric ABC Staining System (Santa Cruz) was used according to manufacturer's instructions.

For von Kossa staining, tissue sections were prepared as described above, rinsed in deionized water, and incubated in 5% silver nitrate solution for 1 hour under direct light (Schott Modulamp), in a reflective chamber. Slides were washed in water, differentiated in 5% sodium thiosulfate pentahydrate for five minutes, rinsed and counterstained for 20 minutes in 1% Alcian blue in 20% acetic acid for visualization of proteoglycan-

rich normal valve tissue. To prevent misidentification of valvular melanocytes as calcium deposits (black, silver-stained areas), neighboring sections were either treated with 0.38M EDTA overnight to dissolve calcium deposits or processed as described above, omitting the silver nitrate step. Quantification of von Kossa reactive area was performed using Image Pro Plus software and calculated as a percentage of von Kossa positive area (black) over total valve section area (blue).

For *In situ* hybridization analysis, the antisense *Osteonectin* probe was obtained from Dr. Katherine Yutzey.[6] Procedures were performed on 10μM-thick frozen sections as previously described.[3]

Echocardiogram

Transthoracic echocardiography was performed on 3, 6, and 12 month old *Sox9$^{flox/+}$;Col2a1-cre* mice and *Sox9$^{fl/+}$* littermate controls using the VisualSonics 770 system (Toronto, Canada) as described.[7] Mice were anesthetized with 1% isoflurane inhalation and placed on a heated platform. Two-dimensional imaging was recorded with a 40-hertz transducer to capture long- and short-axis projections with guided M-Mode, B-Mode and PW Doppler recorded. For each parameter measurement, the average reading was recorded from at least three distinct frames from each of 4-8 animals and the standard deviation calculated. Statistical significance was determined using Student's t-test (P<0.05).

Chick Valve Explant Culture

Mitral valves were dissected from 10-day chick embryos and placed on 10mm-wide 0.1um pore filters (VCWP, Millipore) with culture media (1% chicken embryo extract (Accurate Chemical, USA), 1% Penicillin/Streptomycin, 1 × M199 (Invitrogen), 10% FBS (Invitrogen)). Mitral valve explants from 5-6 embryos were attached to each filter. 1μmol/L retinoic acid in DMSO or DMSO alone (0.001% final concentration) was added after plating and cultures were incubated for 48 hours. Explants were collected in Trizol for RNA isolation or mounted intact to microscope slides and fixed in 4% PFA/PBS for von Kossa staining as described above.

Adenoviral-Sox9 (Ad-Sox9) and adenoviral-GFP (Ad-GFP) were produced according to manufacturer's instructions (AdEasy XL, Stratagene) using the full-length mouse *Sox9* cDNA (for Ad-Sox9) or no insert (Ad-GFP) in pShuttle-IRES-hrGFP-1, purified, and tittered with AdEasy Viral Titer Kit (Stratgene). In Sox9 over-expression experiments Ad-Sox9 or Ad-GFP was applied at 1x10^6 PFU per filter in 50ul serum free culture media for 4 hours, followed by overnight incubation in 1mL serum free culture media prior to RA or DMSO application. Explants were further incubated in 2% serum media for 48 hours and collected for histology and RNA isolation as described above. Statistical significance was determined using Student's t-test on at least 3 independent experiments.

Mouse Valve Explant Culture

Mitral and tricuspid valve structures were dissected from 1-3 day postnatal homozygous *Sox9$^{fl/fl}$*. To prevent de-differentiation, valves were cultured as explants on pore filters as described above for chick valve culture. Adenovirus targeting *Cre Recombinase* (Ad-Cre) (Vector Labs) or GFP (Ad-GFP) was added at 1x10^6 PFU/ per filter in DMEM supplemented with 4mM L-glutamine and 1% Penicillin/Streptomycin. In parallel control experiments, Ad-Cre and Ad-GFP were also added to valve explants from C57/Bl6 wild-type mice). After overnight incubation explants were supplemented with 2% FBS and maintained for an additional 48 hours prior to collection for histology and RNA isolation as described above for chick valve explants. For real-time PCR, statistical significance was determined based on fold changes in Ad-Cre infected *Sox9$^{fl/fl}$* explants relative to Ad-GFP infected littermate controls (n=3). Similar results were observed in Ad-Cre infected wild-type (C57/Bl6) explants (n=2, data not shown).

Online Supplement References

1. Kist R, Schrewe H, Balling R, Scherer G. Conditional inactivation of *Sox9*: A mouse model for campomelic dysplasia. *Genesis*. 2002;32:121-123.

2. Ovchinnikov DA, Deng JM, Ogunrinu G, Behringer RR. *Col2a1*-directed expression of cre recombinase in differentiating chondrocytes in transgenic mice. *Genesi*s. 2000;26:145-146.

3. Lincoln J, Kist R, Scherer G, Yutzey KE. Sox9 is required for precursor cell expansion and extracellular matrix organization during mouse heart valve development. *Developmental Biology*,. 2007;305:120-132.

4. Sanes JR, Rubenstein JL, Nicolas JF. Use of a recombinant retrovirus to study post-implantation cell lineage in mouse embryos. *EMB*O. 1986;5(12):3133-3142.

5. Stolt CC, Lommes P, Sock E, Chaboissier M, Schedl A, Wegner M. The Sox9 transcription factor determines glial fate choice in the developing spinal cord. *Genes & Developmen*t. 2003;17:1677-1689.

6. Chakraborty S, Cheek J, Sakthivel B, Aronow BJ, Yutzey KE. Shared gene expression profiles in developing heart valves and osteoblast progenitor cells. *Physiol Genomics*. 2008;35:75-85.

7. Levay AK, Peacock JD, Lu Y, Koch M, Hinton RB,Jr, Kadler KE, Lincoln J. Scleraxis is required for cell lineage differentiation and extracellular matrix remodeling during murine heart valve formation in vivo. *Circ Re*s. 2008;103:948-956.

8. Yang X, Fullerton DA, Su X, Ao L, Cleveland Jr JC, Meng X. Pro-osteogenic phenotype of human aortic valve interstitial cells is associated with higher levels of toll-like receptors 2 and 4 and enhanced expression of bone morphogenetic protein 2. *J Am Coll Cardiol*. 2009;53:491-500.

9. Pohjolainen V, Taskinen P, Soini Y, Rysä J, Ilves M, Juvonen T, Ruskoaho H, Leskinen H, Satta J. Noncollagenous bone matrix proteins as a part of calcific aortic valve disease regulation. *Human Pathology,*. 2008;39:1695-1701.

10. Nigam V, Srivastava D. Notch1 represses osteogenic pathways in aortic valve cells. *J Mol Cell Cardiol*. ;In Press, Uncorrected Proof.

11. Drolet M, Roussel E, Deshaies Y, Couet J, Arsenault M. A high Fat/High carbohydrate diet induces aortic valve disease in C57BL/6J mice. *J Am Coll Cardiol*. 2006;47:850-855.

12. Rajamannan NM, Nealis TB, Subramaniam M, Pandya S, Stock SR, Ignatiev CI, Sebo TJ, Rosengart TK, Edwards WD, McCarthy PM, Bonow RO, Spelsberg TC. Calcified rheumatic valve neoangiogenesis is associated with vascular endothelial growth factor expression and osteoblast-like bone formation. *Circulation*. 2005;111:3296-3301.

13. Rajamannan NM, Subramaniam M, Springett M, Sebo TC, Niekrasz M, McConnell JP, Singh RJ, Stone NJ, Bonow RO, Spelsberg TC. Atorvastatin inhibits hypercholesterolemia-induced cellular proliferation and bone matrix production in the rabbit aortic valve. *Circulation*. 2002;105:2660-2665.

14. Akat K, Borggrefe M, Kaden JJ. Aortic valve calcification - basic science to clinical practice. *Heart*. 2008.

15. Aupperle H, Thielebein J, Kiefer B, März I, Dinges G, Schoon H-. An immunohistochemical study of the role of matrix metalloproteinases and their tissue inhibitors in chronic mitral valvular disease (valvular endocardiosis) in dogs. *The Veterinary Journal,*. ;In Press, Corrected Proof.

16. Rabkin E, Aikawa M, Stone JR, Fukumoto Y, Libby P, Schoen FJ. Activated interstitial myofibroblasts express catabolic enzymes and mediate matrix remodeling in myxomatous heart valves. *Circulation*. 2001;104:2525-2532.

17. Hadian M, Corcoran BM, Han RI, Grossmann JG, Bradshaw JP. Collagen organization in canine myxomatous mitral valve disease: An X-ray diffraction study. *Biophys J*. 2007;93:2472-2476.

18. Hinton R,Jr, Lincoln J, Deutsch G, Osinska H, Manning P, Benson DW, Yutzey K. Extracellular matrix remodeling and organization in developing and diseased aortic valves. *Circ Res*. 2006;98:1431-1438.

19. Joziasse I, van dS, Smith K, Bakkers J, Sieswerda G, Mulder B, Doevendans P. Genes in congenital heart disease: Atrioventricular valve formation. *Basic Res Cardiol*. 2008;103:216-227.

20. Garg V, Muth AN, Ransom JF, Schluterman MK, Barnes R, King IN, Grossfeld PD, Srivastava D. Mutations in NOTCH1 cause aortic valve disease; 10.1038/nature03940. *Natur*e. 2005;437:270-274.

21. Caira F, Stock S, Gleason T, McGee E, Huang J, Bonow R, Spelsberg T, McCarthy P, Rahimtoola S, Rajamannan N. Human degenerative valve disease is associated with up-regulation of low-density lipoprotein receptor-related protein 5 receptor-mediated bone formation. *Journal of the American College of Cardiolog*y. 2006;47:1707-1712.

22. Rajamannan NM, Subramaniam M, Rickard D, Stock SR, Donovan J, Springett M, Orszulak T, Fullerton DA, Tajik AJ, Bonow RO, Spelsberg T. Human aortic valve calcification is associated with an osteoblast phenotype. *Circulatio*n. 2003;107:2181-2184; Epub 2003 Apr 28.

23. Kaden JJ, Bickelhaupt S, Grobholz R, Haase KK, Sarıkoç A, Kılıç R, Brueckmann M, Lang S, Zahn I, Vahl C, Hagl S, Dempfle C, Borggrefe M. Receptor activator of nuclear factor κB ligand and osteoprotegerin regulate aortic valve calcification. *J Mol Cell Cardio*l. 2004;36:57-66.

24. Majumdar R, Miller DV, Ballman KV, Unnikrishnan G, McKellar SH, Sarkar G, Sreekumar R, Bolander ME, Sundt III TM. Elevated expressions of osteopontin and tenascin C in ascending aortic aneurysms are associated with trileaflet aortic valves as compared with bicuspid aortic valves. *Cardiovascular Pathology*,. 2007;16:144-150.

25. Meng X, Ao L, Song Y, Babu A, Yang X, Wang M, Weyant MJ, Dinarello CA, Cleveland JC, Jr., Fullerton DA. Expression of functional toll-like receptors 2 and 4 in human aortic valve interstitial cells: Potential roles in aortic valve inflammation and stenosis. *Am J Physiol Cell Physio*l. 2008;294:C29-35.

26. Moon H-, Choi E, Hyun C. The cardiac sodium-calcium exchanger gene (*NCX-1*) is a potential canine cardiac biomarker of chronic mitral valvular insufficiency. *Journal of Veterinary Internal Medicin*e. 2008;22:1360-1365.

27. Yeghiazaryan K, Skowasch D, Bauriedel G, Schild H, Golubnitschaja O. Could activated tissue remodeling be considered as early marker for progressive valve degeneration- comparative analysis of checkpoint and ECM remodeling gene expression in native degenerating aortic valves and after bioprosthetic replacement. *Amino Acid*s. 2007;32:109-114.

28. Steinmetz MF, Skowasch DF, Wernert NF, Welsch U FAU- Preusse, Clauss,J., FAU PC, Welz AF, Nickenig GF, Bauriedel G. Differential profile of the OPG/RANKL/RANK-system in degenerative aortic native and bioprosthetic valves. *The Journal of heart valve disease JID- 9312096*. 0902.

Online Tables and Figures

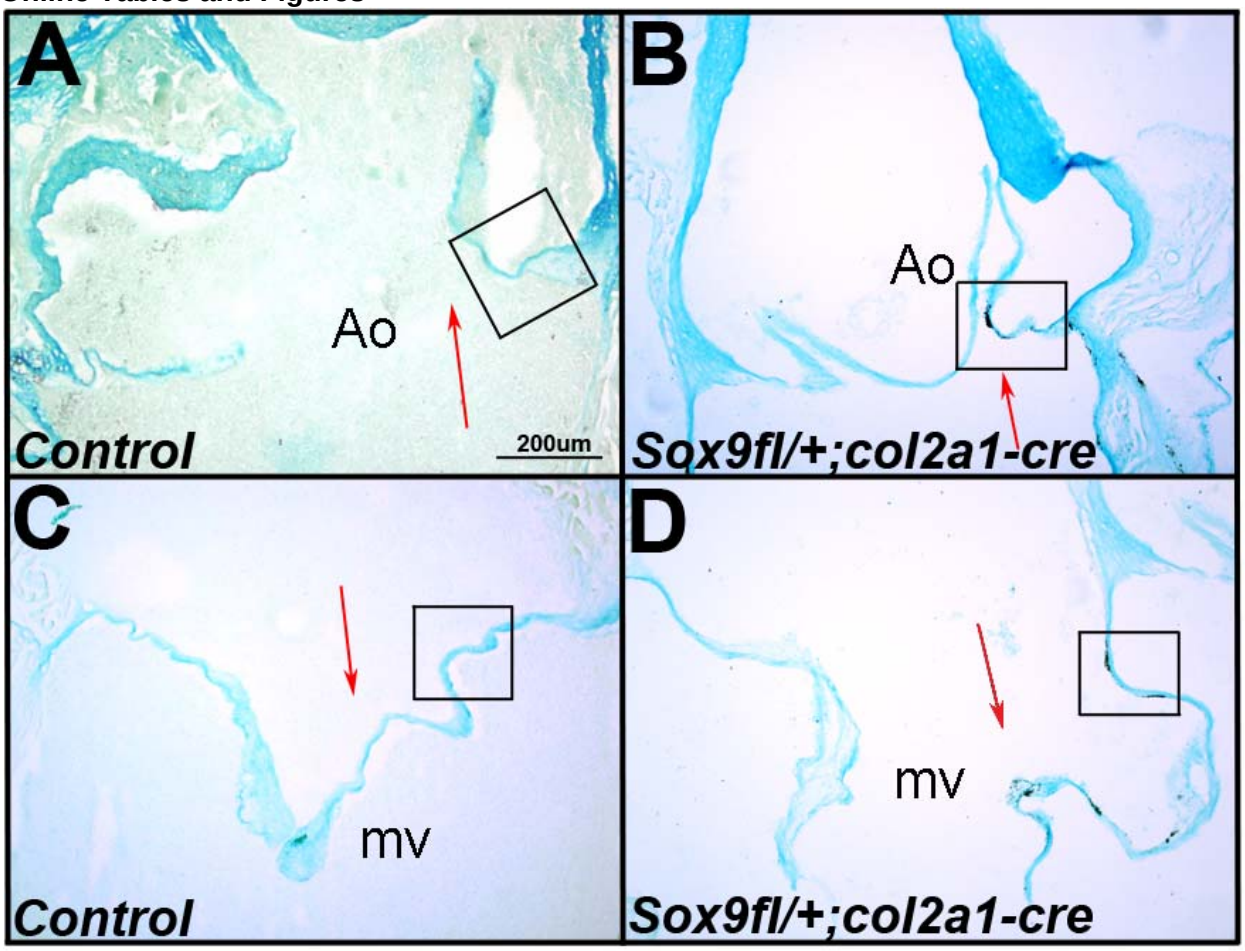

Online Figure I. Lower magnification images corresponding to Figure 2. Calcium deposition was examined by von Kossa reactivity in aortic (Ao) (A, B) and mitral (mv) (C, D) valve leaflets from 12 month old *Sox9$^{fl/+}$;Col2a1-cre* (B, D) and *Sox9$^{fl/+}$* littermate control mice (A, C). Note increased reactivity in *Sox9$^{fl/+}$;Col2a1-cre* mice. Red arrows indicate direction of blood flow; black boxes indicate areas depicted at higher magnification in Figure 2.

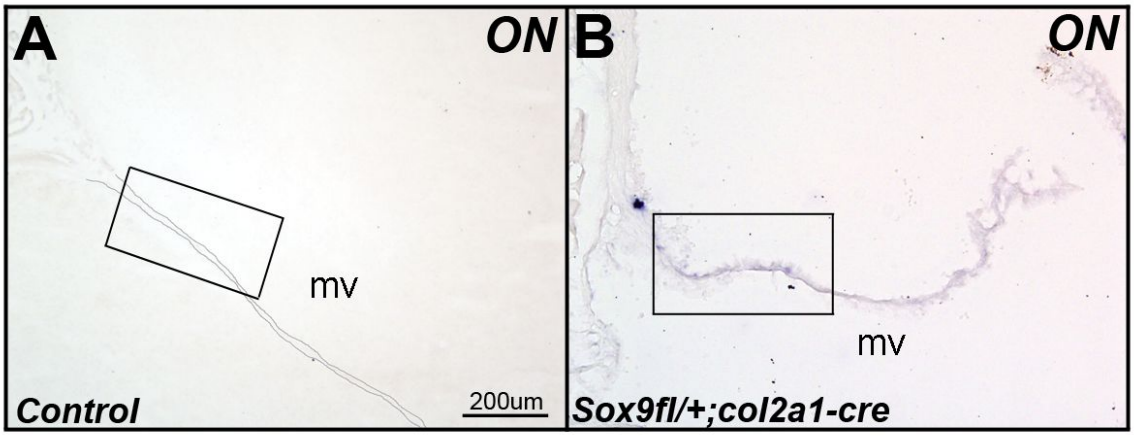

Online Figure II. Lower magnification images corresponding to Figure 3. *In situ* hybridization to determine *Osteonectin* (*ON*) expression in the septal mitral valve leaflet from 12 month old control (*Sox9fl/+)* (A) and *Sox9$^{fl/+}$;Col2a1-cre* (B) mice. Black boxes indicate areas depicted at higher magnification in Figure 3.

Table I **Online 1.**

	Control	*Col2a1cre;Sox9flox/+*	*P value*
IVS;d	0.96 ±0.15	0.86 ±0.21	0.307
LVID;d	4.163 ±0.75	3.75 ±0.47	0.221
LVPW;d	0.94 ±0.14	0.81 ±0.09	0.045
LVID;s	2.45 ±1.09	2.73 ±0.68	0.549
LVPW;s	1.33 ±0.16	1.18±0.15	0.109
LV Vol;d	80.38±33.12	70.55 ±30.85	0.554
LV Vol;s	29.55±20.30	30.77 ±19.50	0.906
%EF	66.32±10.71	54.19 ±23.37	0.186
%FS	36.88±7.528	30.03±11.02	0.161
IVRT	18.05±4.45	18.75 ±2.51	0.324
MV E	883.85±195.81	800.51 ±140.01	0.298
MV A	478.49±237.032	467.36 ±206.84	0.674
MV E/A	1.90 ±0.12	1.73 ±0.20	0.487
AV Peak Vel	835.43 ± 48.38	896.00 ±91.51	0.629
AV Peak Grad	2.86 ±0.34	2.49 ±0.54	0.581

Echocardiography reveals no significant differences in cardiac structure and function in *Sox9$^{flox/+}$;Col2a1-cre* mice compared to *Sox9$^{flox/+}$* controls at 12 months of age. IVS, interventricular septum; LVID, left ventricular internal diameter; LVPW, left ventricular posterior wall thickness; LV Vol, left ventricle volume (μL); RV Vol, right ventricle volume (μL); EF, ejection fraction (percent); FS, fractional shortening (percent); IVRT, isovolumetric relaxation time (ms); MV E, mitral valve E wave peak velocity (mm/s); MV A, mitral valve A wave peak velocity (mm/s); AV Peak Vel, aortic valve peak velocity (mm/s); AV Peak Grad, aortic valve peak pressure gradient (mmHg); d, diastole; s, systole. Values are in mm unless otherwise noted, ±standard deviation

Gene Name	Symbol	3 Months		6 months		12 Months		References
		Fold Change	P-Value	Fold Change	P-Value	Fold Change	P-Value	
Bone morphogenetic protein 10	*Bmp10*	-899.93	0.010	1.48	0.844	3.84	0.199	8
Bone morphogenetic protein 2	*Bmp2*	-1.50	0.407	-1.03	0.961	1.60	0.258	9,10
Cartilage oligomeric matrix protein	*Comp*	-11.23	0.354	-1.58	0.228	2.61	0.043	
Collagen type I α1	*Col1a1*	-1.61	0.161	-1.17	0.655	1.54	0.147	
Collagen type I α2	*Col1a2*	-1.75	0.279	1.24	0.545	1.63	0.101	
Collagen type II α1	*Col2a1*	-10.23	0.281	-331.57	0.047	3.45	0.094	
Collagen type XI α1	*Col11a1*	-1.58	0.700	-1.10	0.851	2.14	0.056	
Colony stimulating factor 1 receptor	*Csf1r*	-1.60	0.274	-1.12	0.670	1.63	0.033	11-18
Colony stimulating factor 2	*Csf2*	-6.39	0.098	-2.73	0.187	9.12	0.054	11-18
Matrilin1	*Matn1*	1.06	0.966	-4.76	0.447	1.61	0.605	
Matrilin2	*Matn2*	-1.44	0.521	-1.25	0.559	1.10	0.716	
Matrix metalloproteinase 14	*Mmp14*	-2.36	0.072	-1.39	0.441	1.34	0.319	
Matrix metalloproteinase 2	*Mmp2*	-1.38	0.510	1.11	0.788	1.30	0.188	15-19
Matrix metalloproteinase 9	*Mmp9*	-2.71	0.097	-1.53	0.412	1.96	0.076	15-19
Noggin	*Nog*	-9.05	0.008	-1.50	0.194	-1.32	0.341	8
Notch gene homolog 1	*Notch1*	-1.51	0.487	-1.03	0.955	1.54	0.246	10, 19, 20
Osteocalcin	*Bglap2*	1.86	0.687	1.16	0.817	2.18	0.096	13, 21-23
Osteonectin	*Sparc*	-1.52	0.266	-1.00	0.997	1.76	0.050	
Osteopontin	*Spp1*	-1.52	0.336	-1.37	0.441	8.68	0.037	9, 12, 21, 22, 24
Platelet/endothelial cell adhesion molecule 1	*Pecam1*	-2.26	0.064	-1.44	0.372	1.34	0.252	
Runx2	*Runx2*	1.26	0.817	-1.25	0.653	2.12	0.018	25
Solute carrier family 8, member 1	*Slc8a1*	-1.43	0.416	1.27	0.698	2.09	0.049	26
Sphingomyelin phosphodiesterase 3	*Smpd3*	-1.56	0.482	-1.09	0.865	1.95	0.036	
Tissue inhibitor of metalloproteinase 1	*Timp1*	-3.27	0.009	1.17	0.603	3.88	0.045	15, 27
Toll-like receptor 2	*Tlr2*	-1.35	0.469	-1.52	0.231	2.11	0.032	8, 25
Tumor necrosis factor superfamily, 11	*Tnfsf11*	-13.33	0.024	-2.29	0.148	3.95	0.037	28
Vascular cell adhesion molecule 1	*Vcam1*	-2.03	0.044	-1.53	0.330	1.87	0.049	

Online Table II. Relative gene transcript levels in *Sox9$^{fl/+}$;Col2a1-cre* mice as compared to *Sox9$^{fl/+}$* littermate controls at 3, 6 and 12 months of age. Quantitative changes in target gene expression following TLDA. Fold changes are calculated as $2^{(-deltaCT)}$, with decreases (fold changes smaller than 1) transformed by dividing from -1 to allow more intuitive interpretation of the data. P-values given were generated by Student's t-test, $p<0.05$ is considered significant. "References" lists citations from published studies indicating significant changes in homologous gene transcript or corresponding protein level in diseased human heart valves, or changes in gene expression in other published mouse models of calcific valve disease.